HAALAND, A. & NILSSON, J. E. (1968). *Acta Chem. Scand.* **22**, 2653–2670.
HEDBERG, L. & HEDBERG, K. (1970). *J. Chem. Phys.* **53**, 1228–1234.
JOHNSON, C. K. (1965). *ORTEP*. Report ORNL-3794. Oak Ridge National Laboratory, Tennessee.
KEALY, T. J. & PAUSON, P. L. (1951). *Nature (London)*, **168**, 1039–1040.
LAUHER, J. W., ELIAN, M., SUMMERVILLE, R. H. & HOFFMAN, R. (1976). *J. Am. Chem. Soc.* **98**, 3219–3224.
MAXWELL, W. M., WEISS, R., SINN, E. & GRIMES, R. N. (1977). *J. Am. Chem. Soc.* **99**, 4016–4029.
MILLER, S. A., TEBBOTH, J. A. & TREMAINE, J. F. (1952). *J. Chem. Soc.* pp. 632–635.
OGASAHARA, K., SORAI, M. & SUGA, H. (1979). *Chem. Phys. Lett.* **68**, 457–460.
PAULUS, E., HOPPE, W. & HUBER, R. (1967). *Naturwissenschaften*, **54**, 67–68.
PIPAL, J. R. & GRIMES, R. N. (1978). *Inorg. Chem.* **17**, 10–14.
PIPAL, J. R. & GRIMES, R. N. (1979). *Inorg. Chem.* **18**, 1936–1940.
SALZER, A. & WERNER, H. (1972*a*). *Angew. Chem. Int. Ed. Engl.* **11**, 930–931.
SALZER, A. & WERNER, H. (1972*b*). *Synth. Inorg. Met. Org. Chem.* **2**, 249–258.
SEILER, P. & DUNITZ, J. D. (1979*a*). *Acta Cryst.* B**35**, 1068–1074.
SEILER, P. & DUNITZ, J. D. (1979*b*). *Acta Cryst.* B**35**, 2020–2032.
SEILER, P. & DUNITZ, J. D. (1980). *Acta Cryst.* B**36**, 2255–2260.
SIEBERT, W., BOCHMANN, M., EDWIN, J., KRÜGER, C. & TSAY, Y.-H. (1978). *Z. Naturforsch. Teil B*, **33**, 1410–1416.
SIEBERT, W., BÖHLE, C. & KRÜGER, C. (1980). *Angew. Chem.* **92**, 758–759.
SIEBERT, W., RENK, T., KINBERGER, K., BOCHMANN, M. & KRÜGER, C. (1976). *Angew Chem.* **88**, 850–851.
STEWART, J. M., KRUGER, G. J., AMMON, H. L., DICKINSON, C. & HALL, S. R. (1972). The XRAY system. Computer Science Center, Univ. of Maryland, College Park, Maryland.
STEWART, R. F., DAVIDSON, E. R. & SIMPSON, W. T. (1965). *J. Chem. Phys.* **42**, 3175–3187.
TAKUSAGAWA, F. & KOETZLE, T. F. (1979). *Acta Cryst.* B**35**, 1074–1081.
TUGGLE, R. M. & WEAVER, D. L. (1971). *Inorg. Chem.* **10**, 1504–1510.
WATERS J. M. & IBERS, J. A. (1977). *Inorg. Chem.* **16**, 3273–3277.
WERNER, H. & SALZER, A. (1972). *Synth. Inorg. Met. Org. Chem.* **2**, 239–248.

Acta Cryst. (1983). B**39**, 612–620

Magnetic Properties and X-ray Crystal Structure of Tris(4-morpholinecarbodithioato)iron(III)–Dichloromethane at 20, 110, 178 and 293 K*

BY KENNY STÅHL

Inorganic Chemistry 2, Chemical Center, University of Lund, PO Box 740, S-22007 Lund, Sweden

(*Received* 8 *March* 1983; *accepted* 6 *June* 1983)

Abstract

The crystal structure of $Fe(S_2CNC_4H_8O)_3.CH_2Cl_2$, $M_r = 627{\cdot}51$, has been determined from X-ray four-circle single-crystal diffractometer data at 20 (2), 110 (2), 178 (2) and 293 (1) K. Refinements converged to R values of 0·055, 0·062, 0·061 and 0·041 for 1320, 2720, 2048 and 1601 reflexions, respectively. The crystal structure shows a phase transition at ~150 K, both phases being triclinic with space group $P\bar{1}$ and $Z = 2$. The complexes are mononuclear with pseudosymmetry D_3 and are van der Waals packed. The dichloromethane molecules are located close to the FeS_6 core of the complexes and show some evidence of hydrogen bonding to S. The magnetic properties were investigated with the Faraday method and μ_{eff} varies between 3·80 (2) at 20 K and 5·60 (6) BM at 293 K (1 BM = $9{\cdot}274 \times 10^{-24}$ J T^{-1}). The geometry of the FeS_6 core shows the same correlation to μ_{eff} as do other tris(dithiocarbamato)iron(III) structures. The intermediate μ_{eff} at low temperatures is explained by a change in crystal packing and hydrogen bonding at the phase transition. Earlier explanations (a spin quartet ground state, strong hydrogen-bond interaction, cooperative effects, and desolvation) are invalidated.

Introduction

The magnetic behaviour of most substituted tris(dithiocarbamoto)iron(III) [Fe(dtc)$_3$] compounds can be described as a thermal equilibrium between the low-spin doublet and the high-spin sextet states of iron(III). The effective magnetic moment, μ_{eff}, is thus expected to vary between ~2 BM (1 BM = $9{\cdot}274 \times 10^{-24}$ J T^{-1}) (the low-temperature limit) and 5·92 BM (the high-temperature limit). In the case of tris(4-morpholinecarbodithioato)iron(III)–dichloromethane the μ_{eff} *vs* T curve is intermediate between that for a pure high-spin compound and that with a complete high-spin to low-spin transition (Fig. 1*a*). This anomalous behaviour has been subject to numerous investigations (Butcher & Sinn, 1976*a*,*b*; Butcher, Ferraro & Sinn, 1976; Rinninger, Duffy, Weir, Gelerinter, Stanford & Uhrich, 1977; Haddad, Federer, Lynch & Hen-

* Compounds with Intermediate Spin. 8. Part 7: Ståhl & Ymén (1983).

0108-7681/83/050612-09$01.50

drickson, 1980; Eisman, Reiff, Butcher & Sinn, 1981; Duffy, Lockhart, Gelerinter, Todoroff & Uhrich, 1981; Malliaris & Papaefthimiou, 1982); the room-temperature crystal structure was solved by Healy & Sinn (1975). Four explanations have been discussed:

(1) A strong tetragonal distortion, giving a quartet ground state with $\mu_{eff} \approx 4$ BM as the low-temperature limit (Butcher & Sinn, 1976*a*). Mössbauer spectroscopic investigations have subsequently invalidated this explanation (Eisman *et al.*, 1981).

(2) Hydrogen bonds are formed between the dichloromethane solvate molecule and S atoms in the FeS_6 core, thereby weakening the Fe–S bonds and stabilizing the high-spin state (Butcher, Ferraro & Sinn, 1976).

(3) Cooperative effects (Haddad, Lynch, Federer & Hendrickson, 1981; Haddad, Federer, Lynch & Hendrickson, 1981). When the transition from high to low spin involves formation of small domains in the low-spin state, a large number of crystal defects (*e.g.* induced by grinding) will favour domain nucleation, but will hinder domain growth, resulting in a more gradual spin transition, which is not always completed (Fig. 1*b*). It has been questioned if this description is applicable to the present type of system (Duffy *et al.*, 1981; Albertsson, Oskarsson & Ståhl, 1982).

(4) The title compound is purely high spin, and the observed behaviour is an effect of desolvation (Malliaris & Papaefthimiou, 1982).

This paper reports the X-ray crystal structure of tris(4-morpholinecarbodithioato)iron(III)–dichloromethane at 20 (2), 110 (2), 178 (2) and 293 (1) K and its magnetic moment between 3 and 300 K. The magnetic properties are discussed in view of the molecular geometry and the change in crystal packing in connexion with an observed phase transition. The above proposed explanations are shown to be without importance in determining the magnetic properties of the title compound.

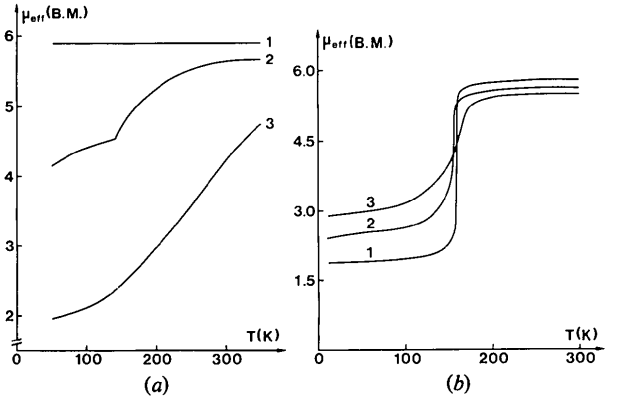

Fig. 1. (*a*) Effective magnetic moment *vs* temperature: (1) tris(pyrrolidinecarbodithioato)iron(III), (2) tris(4-morpholinecarbodithioato)iron(III)–CH_2Cl_2 (title compound), (3) tris(*N*,*N*-dimethyldithiocarbamato)iron(III). (*b*) Effective magnetic moment *vs* temperature for $[Fe(3\text{-}OCH_3\text{-saleen})_2]PF_6$: (1) as-grown microcrystalline solid, (2) sample ground with mortar and pestle, (3) sample ground in ball mill (from Haddad, Federer, Lynch & Hendrickson, 1981).

Experimental

Preparation: The title compound was prepared in dry N_2 atmosphere by adding morpholine and a 0·1 *M* solution of anhydrous iron(III) chloride in ethanol to a solution of 0·3 *M* sodium hydroxide and 0·3 *M* carbon disulphide in ethanol. Black single crystals were grown from dichloromethane solutions by slow evaporation at room temperature. The crystal system is triclinic, space group $P\bar{1}$, with $Z = 2$. All crystals used were tabular $(01\bar{1})$ bounded by $\{011\}$ and $\{2\bar{1}1\}$.

Data collection was made with an Enraf–Nonius CAD-4 diffractometer using Mo $K\alpha$ radiation. Temperatures between 100 and 273 K were attained with a gas-stream apparatus working with $N_2(l)$ (Danielsson, Grenthe & Oskarsson, 1976). The regulating thermocouple was calibrated with an Omega Eng. Hyp-O probe (0·2 mm diameter) in place of the crystal. The 20 K data set was collected using a Be-walled conduction-cooling He(*l*) cryostat (Albertsson, Oskarsson & Ståhl, 1979). The measuring temperatures were estimated as 20 (2), 110 (2), 178 (2) and 293 (1) K, respectively. A reflexion was measured if $I \geq 3\sigma_c(I)$ in the pre-scan [$\sigma_c(I)$ is based on counting statistics]. Maximum counting time was 120 s and the requested $\sigma_c(I)/I$ in the final scan was 0·030.

At 110, 178 and 293 K data were collected from a complete half-sphere with $\theta < 25°$ ($|h| \leq 15$, $|k| \leq 12$, $|l| \leq 13$). In order to cover a complete half-sphere at 20 K with the restricted κ movement ($|\kappa| < 60°$) of the Be cryostat, three crystals with different orientations were used. For the second and third crystals only reflexions with a calculated minimum intensity corresponding to $|F| > 20$ and in the θ interval 12·5 to 40° were measured ($|h| \leq 18$, $|k| \leq 17$, $|l| \leq 17$). Two (at 20 and 110 K) or three control reflexions were measured every 2 h. They showed no systematic intensity variations.

Unit-cell dimensions (Table 1 and Fig. 2*a*) were determined by least-squares refinements from 50 reflexions with $6° < \theta < 20°$. One series was measured with the temperature decreasing and one with the temperature increasing in order to reveal hysteresis effects. The phase transition at ~150 (3) K was further investigated with rotational and Weissenberg photographs taken at 125 (2) and 293 (4) K. Information concerning data collection, reduction and structure refinements are given in Table 1.

Data reduction: Corrections were made for Lorentz, polarization and absorption effects. The 20 K data set

Table 1. *Crystal data, collection and reduction of intensity data and least-squares-refinement details [space group $P\bar{1}$ with $Z = 2$, $M_r = 627{\cdot}51$ and $F(000) = 646$]*

Temperature (K)	293 (1)	178 (2)	110 (2)	20 (2)
a (Å)	13·094 (3)	12·918 (5)	12·926 (3)	12·846 (10)
b (Å)	10·686 (2)	10·618 (3)	10·546 (2)	10·515 (4)
c (Å)	11·495 (2)	11·397 (4)	11·337 (2)	11·287 (4)
α (°)	116·05 (1)	115·59 (2)	115·42 (1)	115·29 (4)
β (°)	105·05 (2)	104·55 (5)	105·03 (3)	104·94 (4)
γ (°)	99·44 (2)	100·23 (3)	100·45 (2)	100·64 (4)
V (Å^3)	1321 (1)	1289 (2)	1270 (1)	1254 (2)
D_x (Mg m^{-3})	1·578 (1)	1·617 (3)	1·641 (1)	1·662 (3)
Graphite monochromator	Yes	Yes	Yes	No (Zr filter)
Crystal size (mm)	0·4 × 0·25 × 0·1	0·4 × 0·25 × 0·1	0·4 × 0·4 × 0·2	0·4 × 0·3 × 0·06 0·4 × 0·3 × 0·1
μ ($\lambda = 0{\cdot}71069$ Å) (mm^{-1})	1·24	1·27	1·30	1·31
Range of transmission factor	0·69–0·89	0·69–0·89	0·70–0·80	0·77–0·88
ω–2θ scan width, $\Delta\omega$ (°)	0·7 + 0·5 tan θ	0·7 + 0·5 tan θ	1·0 + 0·5 tan θ	1·0 + 0·5 tan θ
No. of reflexions				
recorded	4819	4644	5103	3606
considered not observable	3125	2488	1894	1891
in final LS cycle, m	1601	2048	2720	1320
No. of parameters refined, n	280	280	298	298
R	0·041	0·061	0·062	0·055
wR	0·054	0·083	0·086	0·067
$S = [\sum w\lvert\Delta F\rvert^2/(m-n)]^{1/2}$	2·07	3·53	1·29	2·35
c_1 (in weighting function)	0·020	0·017	0·050	0·000
c_2 (in weighting function)	–	–	1·20	1·00

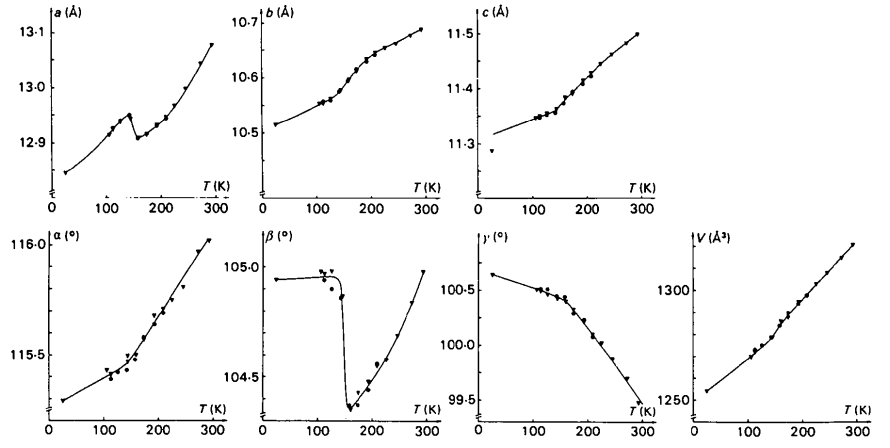

(*a*)

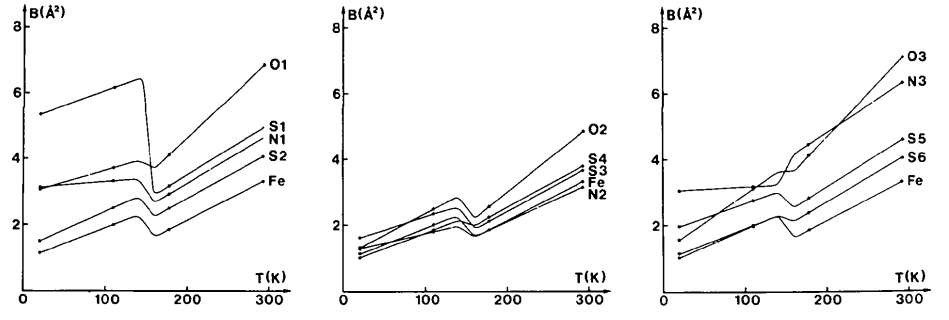

(*b*)

Fig. 2. (*a*) Unit-cell dimensions *vs* temperature. ▼ Measured with successively decreasing temperature. ● Measured with successively increasing temperature. (*b*) Isotropic mean temperature factor coefficients *vs* temperature.

was also corrected for absorption in the Be walls and the 250 reflexions with $\theta < 12{\cdot}5°$ were excluded in order to avoid interference from the powder background of the Be walls (Albertsson, Oskarsson & Ståhl, 1979). Friedel pairs were averaged in all data sets before structure refinement commenced.

Refinement of the structures: Parameters from Healy & Sinn (1975) were used to start the refinement of the 293 K structure. The function $\sum w(\Delta F)^2$ was minimized with full-matrix least-squares refinement. The weights, w, were calculated from $w^{-1} = \sigma_c^2(|F_o|) + (c_1|F_o|)^2 + c_2$, with c_1 and c_2 adjusted to give constant $\langle w(\Delta F)^2 \rangle$ in different $|F_o|$ and $\sin\theta$ intervals. Only parameters of non-H atoms were refined. The coordinates of the H atoms were recalculated between every second least-squares (LS) cycle from geometrical considerations. They were all given isotropic temperature factor coefficients ~25% greater than the isotropic mean value for the adjacent C atom.

There is a disorder of the dichloromethane molecules at 20 and 110 K (see below) and it was possible to refine alternative (*A* and *B*) sites of the C and Cl(1) atoms. Their occupancy factors were determined in separate refinements of dichloromethane and were kept constant in the final LS cycles.

The number of reflexions in the 20 and 293 K data sets are low, about 4·4 reflexions per refined parameter, although no anomalous heavy-atom dependence was found; $R = 0{\cdot}27$ including only Fe, S and Cl, while the final value of R is 0·041. The 20 K anisotropic thermal parameters of N(1), C(3), C(12), O(3) and C(*B*) are not positive definite, but for each atom the negative eigenvalue is zero within one e.s.d. For these atoms the isotropic mean values are used in the 20 K *ORTEP* drawing (Fig. 3).

The parameter shift/e.s.d. ratios in the last cycle were below 1% (2% at 293 K) or below 2% (5% at 293 K) for morpholine ring No. 3 and the dichloromethane molecule. The final difference maps showed only spurious peaks with maximum heights of 0·6 and 0·7 e Å^{-3} at 293 and 178 K respectively, while the 110 and 20 K data sets also showed some residual peaks of respectively 1·0 and 0·5 e Å^{-3} in the vicinity of the morpholine ring in ligand 3.

Atomic scattering factors and anomalous-dispersion correction factors were taken from *International Tables for X-ray Crystallography* (1974). The computer programs used are described by Lundgren (1982). Fractional coordinates and isotropic mean values of the thermal parameters are given in Table 2.*

* Lists of structure factors, anisotropic thermal parameters, H-atom parameters, selected intramolecular distances and bond angles and packing distances at the four temperatures have been deposited with the British Library Lending Division as Supplementary Publication No. SUP 38639 (55 pp.). Copies may be obtained through The Executive Secretary, International Union of Crystallography, 5 Abbey Square, Chester CH1 2HU, England.

Susceptibility measurement: The magnetic susceptibility was measured on a microcomputer-controlled Cahn RG electrobalance using the Faraday principle (Blom & Hörlin, 1977; Albertsson, Oskarsson & Ståhl, 1982). The samples were polycrystalline and field strengths of 0·4 and 0·8 T were used. To reach temperatures between 3·5 and 77 K a Leybold–Heraeus He(*l*) VNK 3-300 vaporization cryostat was used. The estimated standard deviations of the effective magnetic moment vary between 0·02 BM at 20 K and 0·06 BM at 300 K. Effects of crystallite size, crystal perfection and solvent loss were investigated using different preparations. Measurements were repeated after careful grinding with an agate mortar and pestle and heating the sample to ~363 K in vacuum until complete desolvation.

Investigations of the phase transition: The variations in the unit-cell parameters with temperature (Fig. 2*a*) indicate a phase transition at ~150 K. The curves for b, c, α and γ are continuous but change derivatives and the a and β curves are discontinuous and change derivatives at this temperature. The V curve is almost continuous and its derivative is not significantly changed, pointing to an approximately second-order phase transition. Rotational photographs at 116 K revealed a few additional weak reflexions with $h = \frac{5}{2}$ and $\frac{9}{2}$. The transition to the low-temperature phase, which is also triclinic, is thus accompanied by a doubling of a (the symmetry change is consistent with the approximate second-order phase transition) and a distortion of the unit cell by almost pure shear strain about b^*. The scarcity of the extra reflexions and their low intensities indicate only small deviations from the high-temperature structure. Hence the refinements and the discussion of the low-temperature structure are based on the high-temperature unit cell and space group.

The structure of the high-temperature phase (phase I)

The crystal structure comprises mononuclear complexes with pseudosymmetry D_3, held together by van der Waals forces. Intramolecular distances and angles and some intermolecular distances are given in Tables 3 and 4. Drawings of the complex are shown in Fig. 3. The 293 K parameters were compared with those obtained by Healy & Sinn (1975) by half-normal probability plots of δp (Abrahams & Keve, 1971). Comparison of all parameters results in a slope (k) of 1·52 (1), an intercept (l) of −0·15 (1) and a correlation coefficient (r) of 0·995. Comparison of the coordinates only results in $k = 1{\cdot}67$ (2), $l = -0{\cdot}01$ (1) and $r = 0{\cdot}996$ and of the thermal parameters only results in $k = 1{\cdot}32$ (1), $l = -0{\cdot}13$ (1) and $r = 0{\cdot}992$. This indicates an underestimation of the pooled standard deviations by a factor of about 1·5 and small systematic differences in the thermal parameters that may be

Table 2. *Final atomic coordinates* ($\times 10^4$) *with estimated standard deviations*

$$B_{iso} = \tfrac{4}{3} \sum_i \sum_j \beta_{ij} (\mathbf{a}_i . \mathbf{a}_j).$$

	x	y	z	B_{iso} (Å^2)
(*a*) 20 K				
Fe	2417 (3)	2186 (2)	4819 (2)	1·1 (1)
S(1)	1914 (8)	−78 (4)	4850 (6)	5·3 (3)
S(2)	3591 (5)	874 (3)	3926 (3)	1·5 (1)
C(1)	2844 (23)	−552 (15)	4085 (17)	2·7 (8)
N(1)	3006 (20)	−1883 (11)	3644 (13)	3·1 (7)
C(2)	2544 (23)	−3000 (16)	3937 (16)	2·6 (7)
C(3)	3848 (22)	−2201 (18)	2914 (21)	2·6 (6)
C(10)	2073 (20)	−4530 (14)	2662 (14)	1·5 (6)
C(11)	3345 (23)	−3784 (17)	1720 (29)	3·3 (9)
O(1)	2955 (16)	−4855 (12)	2135 (18)	3·0 (6)
S(3)	3456 (5)	3544 (4)	7282 (4)	1·6 (1)
S(4)	3594 (4)	4469 (3)	5269 (3)	1·0 (1)
C(4)	4107 (18)	4914 (16)	6986 (15)	1·0 (5)
N(2)	4952 (16)	6176 (12)	8031 (12)	1·3 (5)
C(5)	5325 (20)	6559 (16)	9503 (16)	1·7 (6)
C(6)	5623 (19)	7285 (14)	7772 (15)	1·5 (6)
C(12)	5394 (16)	8126 (15)	10424 (14)	1·0 (4)
C(13)	5619 (19)	8816 (15)	8755 (16)	1·4 (6)
O(2)	6102 (13)	9201 (11)	10226 (10)	1·3 (4)
S(5)	744 (5)	2794 (5)	4901 (4)	2·0 (1)
S(6)	1316 (4)	1474 (3)	2482 (3)	1·0 (1)
C(7)	327 (16)	2146 (15)	3096 (14)	1·0 (5)
N(3)	−596 (22)	2164 (17)	2313 (15)	3·1 (8)
C(8)	−1500 (23)	2544 (24)	2793 (19)	2·6 (7)
C(9)	−1099 (33)	1312 (21)	677 (22)	5·0 (1·2)
C(14)	−1950 (29)	3435 (24)	2113 (19)	3·9 (9)
C(15)	−1508 (20)	2214 (21)	156 (17)	2·1 (7)
O(3)	−2415 (13)	2544 (12)	646 (11)	1·6 (4)
C(*A*)*	9359 (30)	8212 (30)	2436 (22)	2·0 (1·0)
C(*B*)	9325 (56)	7791 (32)	1232 (38)	2·4 (1·6)
Cl(1*A*)	8258 (9)	8515 (8)	1420 (11)	2·4 (3)
Cl(1*B*)	8522 (10)	8721 (8)	2220 (11)	0·6 (3)
Cl(2)	9548 (5)	6446 (5)	1388 (4)	2·5 (2)
(*b*) 110 K				
Fe	2418 (1)	2190 (1)	4818 (1)	2·0 (0)
S(1)	1920 (3)	−83 (3)	4844 (3)	6·1 (1)
S(2)	3591 (2)	873 (2)	3914 (2)	2·5 (1)
C(1)	2857 (9)	−566 (9)	4056 (8)	3·4 (3)
N(1)	3029 (8)	−1857 (8)	3622 (7)	3·3 (3)
C(2)	2551 (12)	−2969 (11)	3953 (10)	5·0 (4)
C(3)	3826 (8)	−2233 (11)	2933 (11)	3·6 (4)
C(10)	2120 (8)	−4500 (10)	2695 (9)	3·1 (3)
C(11)	3308 (9)	−3755 (11)	1721 (12)	4·0 (4)
O(1)	2971 (6)	−4801 (7)	2143 (9)	4·7 (3)
S(3)	3459 (2)	3555 (2)	7282 (2)	2·3 (1)
S(4)	3603 (2)	4475 (2)	5277 (2)	1·8 (1)
C(4)	4128 (6)	4921 (8)	7016 (7)	1·4 (2)
N(2)	4943 (5)	6167 (7)	8017 (6)	1·8 (2)
C(5)	5373 (7)	6555 (9)	9516 (8)	2·3 (3)
C(6)	5581 (7)	7258 (9)	7787 (8)	2·1 (3)
C(12)	5396 (7)	8125 (9)	10425 (7)	2·1 (3)
C(13)	5594 (7)	8796 (9)	8775 (8)	2·3 (3)
O(2)	6063 (5)	9166 (6)	10201 (5)	2·5 (2)
S(5)	734 (2)	2781 (3)	4894 (2)	2·7 (1)
S(6)	1311 (2)	1482 (2)	2477 (2)	2·0 (1)
C(7)	330 (7)	2152 (9)	3125 (8)	2·4 (3)
N(3)	−619 (7)	2147 (9)	2313 (7)	3·2 (3)
C(8)	−1501 (10)	2635 (15)	2816 (11)	5·0 (5)
C(9)	−1004 (11)	1371 (15)	765 (10)	4·9 (5)
C(14)	−1980 (9)	3363 (15)	2177 (10)	5·5 (5)
C(15)	−1537 (9)	2172 (13)	207 (9)	4·2 (4)
O(3)	−2419 (5)	2552 (7)	663 (6)	3·1 (2)
C(*A*)†	9365 (13)	8198 (20)	2428 (15)	2·8 (6)
C(*B*)	9225 (17)	7789 (20)	1138 (18)	2·8 (6)
Cl(1*A*)	8262 (4)	8462 (6)	1362 (6)	4·2 (2)
Cl(1*B*)	8515 (5)	8690 (6)	2166 (7)	2·6 (2)
Cl(2)	9553 (3)	6437 (3)	1384 (3)	5·0 (1)
(*c*) 178 K				
Fe	2449 (1)	2162 (2)	4846 (1)	1·8 (1)
S(1)	2018 (3)	−82 (3)	4960 (3)	3·2 (1)
S(2)	3629 (3)	821 (3)	3911 (3)	2·5 (1)
C(1)	2931 (9)	−562 (11)	4126 (10)	2·3 (4)
N(1)	3090 (9)	−1866 (10)	3652 (9)	2·9 (4)
C(2)	2626 (14)	−2966 (13)	4010 (13)	4·0 (5)
C(3)	3867 (11)	−2233 (13)	2908 (13)	3·1 (5)
C(10)	2215 (13)	−4481 (13)	2722 (14)	3·9 (5)
C(11)	3302 (13)	−3800 (14)	1677 (14)	4·2 (6)
O(1)	3005 (8)	−4812 (9)	2126 (10)	4·1 (4)
S(3)	3475 (2)	3572 (3)	7326 (3)	2·1 (1)
S(4)	3618 (3)	4462 (3)	5303 (3)	2·2 (1)
C(4)	4119 (9)	4915 (11)	7044 (10)	1·8 (4)
N(2)	4921 (8)	6173 (9)	8031 (8)	1·9 (3)
C(5)	5303 (12)	6505 (11)	9479 (11)	3·0 (5)
C(6)	5558 (10)	7244 (11)	7778 (11)	2·3 (4)
C(12)	5382 (11)	8161 (11)	10435 (10)	2·6 (4)
C(13)	5563 (12)	8769 (13)	8701 (12)	3·7 (5)
O(2)	6043 (7)	9134 (8)	10191 (7)	2·6 (3)
S(5)	721 (3)	2707 (3)	4887 (3)	2·8 (1)
S(6)	1347 (3)	1455 (3)	2498 (3)	2·4 (1)
C(7)	375 (11)	2126 (13)	3141 (12)	3·3 (5)
N(3)	−528 (10)	2216 (14)	2357 (10)	4·4 (5)
C(8)	−1459 (20)	2639 (28)	2835 (18)	9·3 (1·2)
C(9)	−813 (19)	1635 (29)	870 (17)	9·6 (1·3)
C(14)	−2039 (17)	3148 (25)	2208 (16)	8·6 (1·0)
C(15)	−1499 (15)	2166 (21)	268 (15)	6·7 (8)
O(3)	−2355 (8)	2556 (10)	733 (9)	4·1 (4)
C	9320 (15)	8092 (19)	2274 (17)	6·0 (7)
Cl(1)	8353 (4)	8408 (5)	1278 (5)	7·8 (2)
Cl(2)	9623 (5)	6481 (5)	1424 (5)	7·4 (2)
(*d*) 293 K				
Fe	2478 (1)	2163 (1)	4849 (1)	3·3 (0)
S(1)	2081 (2)	−82 (3)	4972 (3)	4·9 (1)
S(2)	3634 (2)	781 (2)	3880 (2)	4·1 (1)
C(1)	2974 (8)	−549 (9)	4116 (8)	3·9 (4)
N(1)	3150 (7)	−1843 (8)	3670 (8)	4·6 (4)
C(2)	2706 (11)	−2933 (12)	4020 (11)	7·0 (6)
C(3)	3862 (9)	−2257 (11)	2898 (11)	5·7 (5)
C(10)	2247 (11)	−4464 (11)	2750 (13)	6·4 (5)
C(11)	3303 (10)	−3800 (13)	1681 (11)	6·5 (6)
O(1)	3003 (7)	−4804 (8)	2098 (8)	6·8 (4)
S(3)	3506 (2)	3619 (2)	7351 (2)	3·6 (1)
S(4)	3643 (2)	4467 (2)	5323 (2)	3·8 (1)
C(4)	4135 (7)	4925 (8)	7042 (8)	2·6 (3)
N(2)	4902 (6)	6180 (7)	8042 (6)	3·2 (3)
C(5)	5343 (10)	6541 (9)	9496 (9)	5·8 (5)
C(6)	5532 (9)	7248 (10)	7786 (9)	4·9 (4)
C(12)	5384 (10)	8179 (10)	10456 (9)	5·5 (4)
C(13)	5559 (9)	8731 (10)	8694 (9)	5·4 (4)
O(2)	6052 (6)	9123 (6)	10187 (6)	4·8 (3)
S(5)	750 (2)	2704 (3)	4900 (2)	4·7 (1)
S(6)	1351 (2)	1476 (3)	2497 (2)	4·0 (1)
C(7)	397 (9)	2126 (9)	3150 (9)	4·3 (4)
N(3)	−512 (8)	2196 (10)	2390 (8)	6·3 (4)
C(8)	−1380 (17)	2683 (23)	2885 (15)	13·6 (1·2)
C(9)	−818 (15)	1664 (22)	931 (13)	12·6 (1·1)
C(14)	−2070 (13)	3094 (19)	2257 (14)	11·4 (9)
C(15)	−1527 (12)	2098 (17)	324 (12)	9·4 (8)
O(3)	−2337 (7)	2558 (8)	814 (8)	7·1 (4)
C	9262 (15)	8082 (18)	2270 (13)	10·9 (8)
Cl(1)	8410 (4)	8402 (5)	1316 (5)	12·9 (3)
Cl(2)	9638 (4)	6475 (5)	1404 (5)	12·7 (2)

* Occupancies: C(*A*) 0·64 (1), C(*B*) 0·36, Cl(1*A*) 0·61 (1), Cl(1*B*) 0·39.
† Occupancies: C(*A*) 0·54 (1), C(*B*) 0·46, Cl(1*A*) 0·56 (1), Cl(1*B*) 0·44.

caused by differences in the absorption corrections and/or extinction.

The dichloromethane solvate molecules occupy positions close to the FeS_6 core of the complex. The shortest distances are given in Table 3. The sum of the van der Waals radii for the atoms involved are: C···S 3·5 and H···S 3·0 Å (Bondi, 1964). The geometric criterion (Hamilton & Ibers, 1968) thus indicates weak hydrogen bonds between C and S(1) and S(5), while the C—H···S angles, ≤152°, make these bonds somewhat doubtful. The C···S interactions are between centrosymmetrically related pairs of complexes and solvate

molecules and are indicated as broken lines in the packing diagrams (Fig. 4).

The geometry of the S_2CNC_2 groups is in full agreement with those found in other $Fe(dtc)_3$ structures (*cf.* references in Fig. 5), and is not significantly changed between 20 and 293 K. The slight deviations from planarity in the S_2CNC_2 groups and the partial double-bond character in the S–C and C–N bonds indicate a π-bonding system extended over the S_2CN moiety. As seen from the large thermal parameters (Table 2) and the unusually short observed bond distances the morpholine ring in ligand 3 and the dichloromethane molecule are disordered in the high-

Table 3. *Selected intramolecular distances* (Å) *and bond angles* (°) *in the* $Fe[S_2CN(CH_2)_4O]_3$ *complex and the* CH_2Cl_2 *solvate molecule* (*see also Table* 4) *and the shortest distances between* FeS_6 *and* CH_2Cl_2

	293 K	178 K	110 K	20 K
(*a*) The FeS_6 core				
Fe–S(1)	2·443 (3)	2·417 (3)	2·381 (3)	2·366 (5)
Fe–S(2)	2·424 (3)	2·401 (3)	2·372 (2)	2·358 (6)
Fe–S(3)	2·424 (2)	2·397 (3)	2·363 (2)	2·353 (5)
Fe–S(4)	2·418 (3)	2·390 (3)	2·365 (2)	2·353 (4)
Fe–S(5)	2·434 (3)	2·410 (4)	2·383 (2)	2·366 (7)
Fe–S(6)	2·420 (3)	2·392 (3)	2·364 (2)	2·349 (4)
(*b*) Ligand 1				
N(1)–C(2)	1·472 (13)	1·476 (16)	1·461 (13)	1·420 (21)
C(2)–C(10)	1·515 (15)	1·513 (18)	1·495 (13)	1·497 (19)
C(10)–O(1)	1·391 (15)	1·377 (17)	1·419 (12)	1·438 (28)
O(1)–C(11)	1·396 (14)	1·412 (15)	1·421 (13)	1·449 (25)
C(11)–C(3)	1·503 (16)	1·519 (18)	1·467 (14)	1·497 (26)
C(3)–N(1)	1·439 (14)	1·468 (16)	1·459 (13)	1·523 (32)
(*c*) Ligand 2				
N(2)–C(5)	1·462 (11)	1·456 (13)	1·481 (9)	1·449 (18)
C(5)–C(12)	1·589 (12)	1·586 (15)	1·519 (11)	1·497 (20)
C(12)–O(2)	1·414 (12)	1·389 (13)	1·422 (10)	1·448 (19)
O(2)–C(13)	1·498 (11)	1·496 (14)	1·413 (9)	1·452 (18)
C(13)–C(6)	1·453 (13)	1·501 (16)	1·519 (11)	1·517 (19)
C(6)–N(2)	1·477 (12)	1·458 (14)	1·448 (10)	1·496 (20)
(*d*) Ligand 3				
N(3)–C(8)	1·47 (2)	1·50 (3)	1·48 (1)	1·45 (4)
C(8)–C(14)	1·27 (3)	1·26 (3)	1·38 (2)	1·54 (3)
C(14)–O(3)	1·42 (2)	1·43 (2)	1·43 (1)	1·39 (2)
O(3)–C(15)	1·39 (2)	1·39 (2)	1·42 (1)	1·45 (3)
C(15)–C(9)	1·29 (2)	1·34 (3)	1·43 (2)	1·42 (3)
C(9)–N(3)	1·43 (1)	1·44 (2)	1·47 (1)	1·55 (3)
(*e*) CH_2Cl_2				
C(*A*)–Cl(1*A*)	1·54 (2)	1·65 (2)	1·76 (2)	1·75 (3)
C(*B*)–Cl(1*B*)			1·74 (2)	1·82 (6)
C(*A*)–Cl(2)	1·79 (2)	1·74 (2)	1·83 (2)	1·83 (3)
C(*B*)–Cl(2)			1·67 (2)	1·56 (4)
Cl(1*A*)–C(*A*)–Cl(2)	116 (1)	116 (1)	110 (1)	112 (1)
Cl(1*B*)–C(*B*)–Cl(2)			114 (1)	116 (3)
(*f*) $FeS_6\cdots CH_2Cl_2$				
S(1)–C(*A*)	3·67 (2)	3·52 (2)	3·25 (2)	3·23 (3)
S(1)–H(1C*A*)	2·82	2·72	2·47	2·46
S(1)–H(1C*A*)–C(*A*)	136	133	130	129
S(5)–C(*A*)	3·70 (1)	3·69 (2)	3·63 (2)	3·61 (2)
S(5)–H(2C*A*)	2·80	2·76	2·68	2·66
S(5)–H(2C*A*)–C(*A*)	145	148	150	151
S(6)–C(*B*)	4·03 (2)	3·90 (2)	3·70 (2)	3·65 (4)
S(6)–H(1C*B*)	3·18	3·01	2·75	2·72
S(6)–H(1C*B*)–C(*B*)	140	144	152	147

Table 4. *Some average geometric parameters of the* FeS_6 *core and the* S_2CNC_2 *part of the ligands*

Temperature (K)	293 (1)	178 (2)	110 (2)	20 (2)
μ_{eff} (BM)	5·60 (6)	5·05 (4)	4·45 (3)	3·80 (2)
⟨Fe–S⟩ (Å)*	2·427 (3)	2·401 (4)	2·371 (2)	2·358 (5)
⟨S–Fe–S⟩ (°)*	72·7 (1)	73·4 (1)	74·0 (1)	74·2 (2)
⟨S···S⟩ (Å)*	2·873 (3)	2·869 (4)	2·854 (3)	2·844 (7)
Edge of triangular faces (Å)*	3·536 (4)	3·496 (5)	3·455 (3)	3·436 (7)
Height of prism (Å)	2·620 (4)	2·595 (5)	2·560 (3)	2·532 (6)
Trigonal twist, α (°)*	33·5 (3)	34·9 (3)	36·7 (3)	37·1 (3)
Tilt between triangular faces (°)*	3 (1)	3 (1)	3 (1)	3 (1)
⟨S–C⟩ (Å)*	1·715 (9)	1·719 (11)	1·722 (9)	1·710 (18)
⟨S–C–S⟩ (°)*	114·1 (5)	113·1 (6)	112·0 (4)	111·9 (9)
⟨C–N⟩ (Å)*	1·322 (12)	1·325 (15)	1·319 (10)	1·327 (23)
⟨N–C⟩ (Å)*	1·457 (15)	1·467 (18)	1·467 (12)	1·477 (30)
⟨C–N–C⟩ (°)*	112·8 (9)	114 (1)	112·7 (8)	112 (1)
R.m.s. deviation from the S_2CNC_2 planes (Å)	0·0141	0·0199	0·0211	0·0266

* Tabulated e.s.d.'s are r.m.s. values from the individual e.s.d.'s.

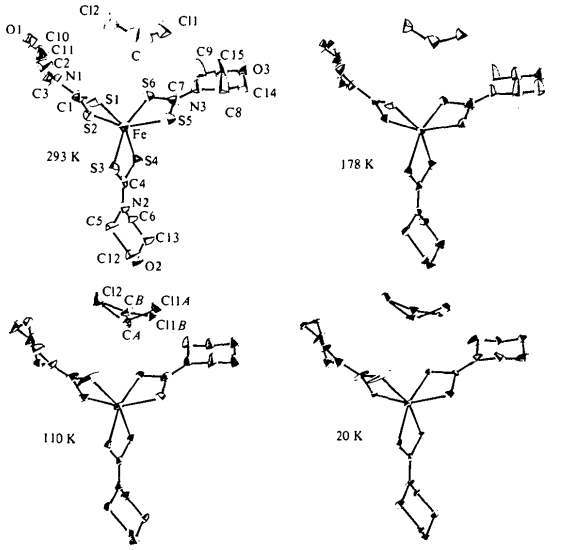

Fig. 3. Drawings of tris(4-morpholinecarbodithioato)iron(III)–CH_2Cl_2 viewed along the pseudo threefold axis. CH_2Cl_2 is in the same plane as the complex. The thermal ellipsoids are scaled to include 50% probability.

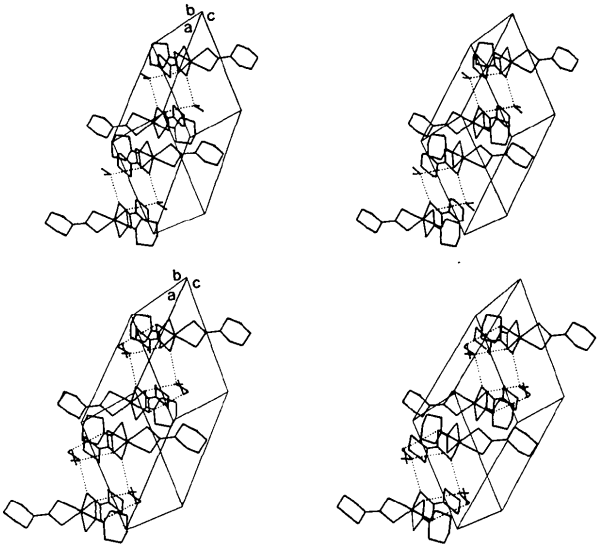

Fig. 4. Stereoscopic drawings of the crystal packing of tris(4-morpholinecarbodithioato)iron(III)–CH_2Cl_2 above and below the phase-transition temperature. C···S interactions are indicated as broken lines.

temperature phase. Because of the high degree of disorder no bond-length corrections based on thermal motions have been applied.

The structure of the low-temperature phase (phase II)

Inspection of the packing diagrams (Fig. 4) and the coordinate list (Table 2) reveals the main changes in the phase transition to be in the morpholine ring in ligand 3 and in the dichloromethane molecule. The change in the morpholine ring is due to decreased disorder in the low-temperature phase as seen from the decrease in thermal parameters and increased observed bond lengths. The dichloromethane molecules are distributed between two sites below the phase transition temperature. Site *A* [Cl(1*A*)–C(*A*)–Cl(2)] is approximately the same as that of the high-temperature phase, while site *B* [Cl(1*B*)–C(*B*)–Cl(2)] corresponds to a re-orientation of the dichloromethane molecule. As seen from Table 3 site *B* gives a new possible hydrogen bond, C(*B*)···S(6). The C(*A*)···S(1) distance becomes remarkably short in the low-temperature phase, but this may partly be an artefact due to unresolved disorder of S(1).

Thermal parameters and the geometry of the FeS_6 core

The thermal parameters (Table 2, Fig. 2*b*) are unusually large at 20 K. B_{iso} is typically 0·5 to 1·0 Å^2 in comparable X-ray crystal structures at 20 to 30 K (Albertsson, Oskarsson, Ståhl, Svensson & Ymén, 1980, 1981), while this investigation shows values mainly between 1·0 and 5·0 Å^2. At 20 K this difference cannot be explained by larger thermal motions. The explanation lies in different kinds of unresolved features of the low-temperature phase, *i.e.* disorder of the morpholine ring in ligand 3, effects from the two dichloromethane orientations and effects of a mixture of high- and low-spin complexes. The C···S interactions propagate the (resolved) disorder of the dichloromethane molecule into the complex and especially to S(1), which is involved in the strongest C···S interaction. At magnetic moments between ~2 and 5·92 BM $Fe(dtc)_3$ crystal structures consist of a mixture of the high- and low-spin forms of the complex. The low-spin molar ratio, $x_{l.s.}$, is defined by

$$\mu_{eff}^2 = x_{l.s.}(\mu_{eff}^{l.s.})^2 + (1 - x_{l.s.})(\mu_{eff}^{h.s.})^2. \quad (1)$$

$(\mu_{eff}^{h.s.})^2 = 35$ and

$$(\mu_{eff}^{l.s.})^2 = \left[8 + \left(3\frac{Z}{RT} - 8\right)\exp\left(-\frac{3}{2}\frac{Z}{RT}\right)\right] \Bigg/ \left\{\frac{Z}{RT}\left[2 + \exp\left(-\frac{3}{2}\frac{Z}{RT}\right)\right]\right\}$$

where Z is the spin orbit coupling constants (Earnshaw, 1968). At 20, 110, 178 and 293 K $x_{l.s.}$ is 0·65 (1), 0·49 (1), 0·32 (1) and 0·10 (1), respectively. From plots of the average Fe–S distances, S–Fe–S angles, and trigonal twist of the FeS_6 polyhedron (α) *vs* μ_{eff} for 27 $Fe(dtc)_3$ crystal structures (Fig. 5) one can estimate the differences between pure high-spin and pure low-spin complexes: Δ(Fe–S) ≈ 0·15 Å, Δ(S–Fe–S)

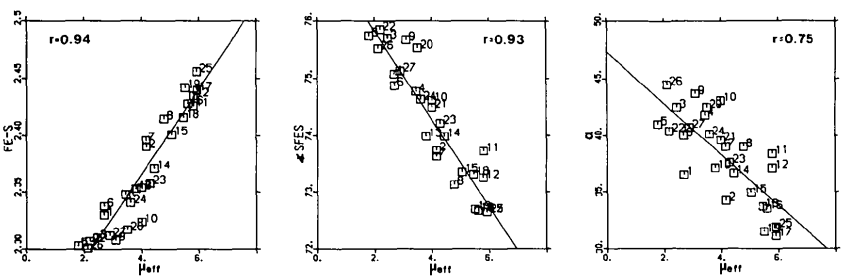

No.	Substituents	Solvate	Temperature (K)	Reference
1	Dihydroxyethyl	—	175	(*a*)
2	Dihydroxyethyl	—	295	(*a*)
3	Dibenzyl	—	175	(*b*)
4	Dibenzyl	—	295	(*b*)
5	Dimethyl	—	25	(*c*)
6	Dimethyl	—	175	(*d*)
7	Dimethyl	—	295	(*d*)
8	Dimethyl	—	400	(*c*)
9	Dipropionitrile	½$CHCl_3$	178	(*e*)
10	Dipropionitrile	½$CHCl_3$	298	(*e*)
11	Tetramethylene	½C_6H_6	175	(*f*)
12	Tetramethylene	½C_6H_6	295	(*f*)
13	Morpholinyl	CH_2Cl_2	20	(*g*)
14	Morpholinyl	CH_2Cl_2	110	(*g*)
15	Morpholinyl	CH_2Cl_2	178	(*g*)
16	Morpholinyl	CH_2Cl_2	293	(*g*)
17	Morpholinyl	CH_2C_2	293	(*h*)
18	Morpholinyl	$CHCl_3$	300	(*i*)
19	Morpholinyl	H_2O	300	(*i*)
20	Morpholinyl	$2C_6H_6$	300	(*j*)
21	Morpholinyl	$C_6H_5NO_2$	300	(*k*)
22	Diethyl	—	79	(*l*)
23	Diethyl	—	297	(*l*)
24	Dibutyl	C_6H_6	295	(*m*)
25	Tetramethylene	—	295	(*n*)
26	Pyrrole	½CH_2Cl_2	297	(*o*)
27	Methylphenyl	—	300	(*p*)

References: (*a*) Albertsson, Oskarsson & Nygren (1979); (*b*) Albertsson, Elding & Oskarsson (1979); (*c*) Albertsson *et al.* (1981); (*d*) Albertsson & Oskarsson (1977); (*e*) Albertsson, Oskarsson & Ståhl (1982); (*f*) Albertsson & Oskarsson (1982); (*g*) this work; (*h*) Ståhl (1983); (*i*) Butcher & Sinn (1976*a*); (*j*) Butcher & Sinn (1976*b*); (*k*) Cukauskas, Deaver & Sinn (1977); (*l*) Leipoldt & Coppens (1973); (*m*) Mitra, Raston & White (1976); (*n*) Mitra, Raston & White (1978); (*o*) Bereman, Churchill & Nalewajek (1979); (*p*) Healy & White (1972).

Fig. 5. Correlation between structural parameters and effective magnetic moment of substituted $Fe(dtc)_3$ compounds. The probability of 27 randomly distributed observations having a correlation coefficient $r \geq 0{\cdot}487$ is 0·005 (Fisher, 1972).

$\approx 3°$ and $\Delta(\alpha) \approx 10°$. The simultaneous presence of the two spin forms, which cannot be resolved in the present experiment, will increase the observed thermal parameters. Assuming equal occupancy of two Gaussian distributions the increase in B_{iso} can be estimated as

$$\Delta B_{iso} \approx \tfrac{1}{3}8\pi^2(\tfrac{1}{2}\Delta X)^2, \quad (2)$$

where ΔX is the distance between the unresolved positions (Leipoldt & Coppens, 1973). Using the differences between the high- and low-spin forms (origin at Fe) in eq. (2) gives an average $\Delta B_{iso} \approx 0{\cdot}5$ Å^2 for the S atoms, thus largely explaining the increased temperature factor coefficients.

Tables 3 and 4 do not indicate an increased distortion of the FeS_6 core at low temperatures, as had been required in order to have a spin quartet ground state (Butcher & Sinn, 1976*a*). The correlation between the FeS_6 core geometry and μ_{eff} (Fig. 5) fits very well into the behaviour of other $Fe(dtc)_3$ compounds, supporting a doublet–sextet spin equilibrium.

Magnetic properties

Effective magnetic moments *vs* temperature for some tris(4-morpholinecarbodithioato)iron(III) solvates are shown in Fig. 6(*a*). Studies of the magnetic properties of the title compound are complicated by its readiness to lose dichloromethane. To minimize loss of dichloromethane polycrystalline samples containing small ($\leq 0{\cdot}5$ mm) single crystals were used. The resulting μ_{eff} *vs* T curve, *b* in Fig. 6(*a*), shows a distinct break at the phase-transition temperature. The drop in μ_{eff} below 20 K is expected from a completion of the spin transition and/or from zero-field splitting of remaining high-spin

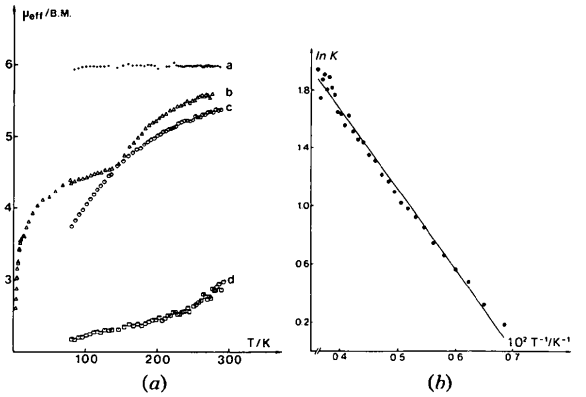

(*a*) (*b*)

Fig. 6. (*a*) Effective magnetic moment *vs* temperature for tris(4-morpholinecarbodithioato)iron(III) solvates: *a* CH_2Cl_2 (phase III), *b* CH_2Cl_2, title compound (phases I and II), *c* desolvated *a*, *b* or *d*, *d* $2C_6H_6$. (*b*) ln K *vs* T^{-1} for tris(4-morpholinecarbodithioato)iron(III)–CH_2Cl_2 phase I [$T > 150$ K, $K = (1 - x_{l.s.})/x_{l.s.}$].

complexes. The curve is fully reproduced even after mild heating (~323 K) in vacuum for several hours. When the crystals were ground and heated to 363 K in vacuum until complete desolvation curve *c* in Fig. 6(*a*) was obtained. Curve *c* is also obtained after desolvating the benzene-solvated tris(morpholinecarbodithioato)-iron(III).

Since grinding of the title compound results in dichloromethane loss it is not possible to investigate directly the cooperative effects on the spin transition (Haddad, Federer *et al.*, 1981; Haddad, Lynch *et al.*, 1981). However, the distinct and reproducible μ_{eff} *vs* T behaviour at the phase-transition temperature makes it plausible that the sample used was free of the kind of imperfections that it is possible to induce by grinding, and is therefore expected to give the most complete spin transition (*cf.* Fig. 1*b*). Using the closely related phenomenological thermodynamic model established by Gütlich, Köppen, Link & Stanhäuser (1979) it is possible to estimate the strength of the intermolecular interactions in terms of a domain size, n, where $n - 1$ is the number of neighbouring complexes involved in a secondary spin transition induced by the initial one. The n complexes may then act as a nucleus in a continued domain growth:

$$(\text{low-spin complex})_n \rightleftarrows (\text{high-spin complex})_n$$

(Albertsson *et al.*, 1982). Fig. 6(*b*) shows ln K *vs* T^{-1} above the phase-transition temperature. Evaluating the least-squares line gives $\Delta H_{eff} = 4{\cdot}6$ (1) kJ mol^{-1} and $\Delta S_{eff} = 22{\cdot}2$ (4) J K^{-1} mol^{-1}, where $\Delta H_{eff} = n\Delta H°$ and $\Delta S_{eff} = n\Delta S°$. Similar treatment for $Fe(dtc)_3$ in solution results in $\Delta H° = 6$–9 kJ mol^{-1} and $\Delta S° = 17$–23 J K^{-1} mol^{-1} (Evans & James, 1979). This indicates a domain size, n, in the present case, close to unity, and thereby small cooperative effects.

Curve *a* in Fig. 6(*a*) represents a new phase (III) of the same composition as the title compound [triclinic, space group $P\bar{1}$, $Z = 2$, $a = 9{\cdot}264$ (1), $b = 10{\cdot}459$ (1), $c = 13{\cdot}665$ (2) Å, $\alpha = 100{\cdot}65$ (1), $\beta = 95{\cdot}60$ (1), $\gamma = 105{\cdot}83$ (1)° at 293 (1) K], but with the dichloromethane molecules in positions where they cannot give hydrogen bonds to the FeS_6 core (Ståhl, 1983). Desolvation of this phase gave a μ_{eff} *vs* T curve equivalent to curve *c* in Fig. 6(*a*). The existence of this new phase explains the magnetic properties observed by Malliaris & Papaefthimiou (1982).

Thus, in conclusion, neither cooperative effects nor solvent loss are responsible for the intermediate spin behaviour at low temperature of the title compound. The hydrogen bonds are themselves too weak to influence directly the spin state of Fe through weakening and lengthening of the Fe–S distances at any temperature (*cf.* Table 3). Instead the μ_{eff} *vs* T curve (*b* in Fig. 6*a*) shows a close connexion between the magnetic properties and the phase transition, where the changes in crystal packing and hydrogen bonding

below the phase-transition temperature sterically disfavour the low-spin geometry of the complex.

I am indebted to Drs Jörgen Albertsson and Christer Svensson for many stimulating discussions and Ms Lena Timby for part of the susceptibility measurements and drawing of the illustrations. Financial support from the Royal Physiographic Society in Lund and the Swedish Natural Science Research Council is gratefully acknowledged.

References

ABRAHAMS, S. C. & KEVE, E. T. (1971). *Acta Cryst.* A**27**, 157–165.

ALBERTSSON, J., ELDING, I. & OSKARSSON, Å. (1979). *Acta Chem. Scand. Ser. A*, **33**, 703–717.

ALBERTSSON, J. & OSKARSSON, Å. (1977). *Acta Cryst.* B**33**, 1871–1877.

ALBERTSSON, J. & OSKARSSON, Å. (1982). Unpublished results.

ALBERTSSON, J., OSKARSSON, Å. & NYGREN, M. (1979). *Acta Cryst.* B**35**, 1473–1476.

ALBERTSSON, J., OSKARSSON, Å. & STÅHL, K. (1979). *J. Appl. Cryst.* **12**, 537–544.

ALBERTSSON, J., OSKARSSON, Å. & STÅHL, K. (1982). *Acta Chem. Scand. Ser. A*, **36**, 783–795.

ALBERTSSON, J., OSKARSSON, Å., STÅHL, K., SVENSSON, C. & YMÉN, I. (1980). *Acta Cryst.* B**36**, 3072–3078.

ALBERTSSON, J., OSKARSSON, Å., STÅHL, K., SVENSSON, C. & YMÉN, I. (1981). *Acta Cryst.* B**37**, 50–56.

BEREMAN, R. D., CHURCHILL, M. R. & NALEWAJEK, D. (1979). *Inorg. Chem.* **18**, 3112–3117.

BLOM, B. & HÖRLIN, T. (1977). *Chem. Commun. Univ. Stockholm* No. 5.

BONDI, A. (1964). *J. Phys. Chem.* **68**, 441–451.

BUTCHER, R. J., FERRARO, J. R. & SINN, E. (1976). *J. Chem. Soc. Chem. Commun.* pp. 910–912.

BUTCHER, R. J. & SINN, E. (1976*a*). *J. Am. Chem. Soc.* **98**, 5159–5168.

BUTCHER, R. J. & SINN, E. (1976*b*). *J. Am. Chem. Soc.* **98**, 2440–2449.

CUKAUSKAS, E. J., DEAVER, B. S. JR & SINN, E. (1977). *J. Chem. Phys.* **67**, 1257–1266.

DANIELSSON, S., GRENTHE, I. & OSKARSSON, Å. (1976). *J. Appl. Cryst.* **9**, 14–17.

DUFFY, N. V., LOCKHART, T. E., GELERINTER, E., TODOROFF, D. & UHRICH, D. L. (1981). *Inorg. Nucl. Chem. Lett.* **17**, 1–4.

EARNSHAW, A. (1968). *Introduction to Magnetochemistry*. London: Academic Press.

EISMAN, G. A., REIFF, W. M., BUTCHER, R. J. & SINN, E. (1981). *Inorg. Chem.* **20**, 3484–3486.

EVANS, D. F. & JAMES, T. A. (1979). *J. Chem. Soc. Dalton Trans.* pp. 723–726.

FISHER, R. A. (1972). *Statistical Methods for Research Workers*. London: Hafner Press.

GÜTLICH, P., KÖPPEN, H., LINK, R. & STEINHÄUSER, H. G. (1979). *J. Chem. Phys.* **70**, 3977–3983.

HADDAD, M. S., FEDERER, W. D., LYNCH, M. W. & HENDRICKSON, D. N. (1980). *J. Am. Chem. Soc.* **102**, 1468–1470.

HADDAD, M. S., FEDERER, W. D., LYNCH, M. W. & HENDRICKSON, D. N. (1981). *Inorg. Chem.* **20**, 131–139.

HADDAD, M. S., LYNCH, M. W., FEDERER, W. D. & HENDRICKSON, D. N. (1981). *Inorg. Chem.* **20**, 123–131.

HAMILTON, W. C. & IBERS, J. A. (1968). In *Hydrogen Bonding in Solids*. New York: Benjamin.

HEALY, P. C. & SINN, E. (1975). *Inorg. Chem.* **14**, 109–115.

HEALY, P. C. & WHITE, A. H. (1972). *J. Chem. Soc. Dalton Trans.* pp. 1163–1171.

International Tables for X-ray Crystallography (1974). Vol. IV. Birmingham: Kynoch Press.

LEIPOLDT, J. G. & COPPENS, P. (1973). *Inorg. Chem.* **12**, 2269–2274.

LUNDGREN, J.-O. (1982). *Crystallographic Computer Programs*. Report No. UUIC-B13-4-05. Univ. of Uppsala.

MALLIARIS, A. & PAPAEFTHIMIOU, V. (1982). *Inorg. Chem.* **21**, 770–774.

MITRA, S., RASTON, C. & WHITE, A. H. (1976). *Aust. J. Chem.* **29**, 1899–1904.

MITRA, S., RASTON, C. & WHITE, A. H. (1978). *Aust. J. Chem.* **31**, 547–553.

RINNINGER, D. P., DUFFY, N. V., WEIR, R. C., GELERINTER, E., STANFORD, J. & UHRICH, D. L. (1977). *Chem. Phys. Lett.* **52**, 102–106.

STÅHL, K. (1983). *Inorg. Chim. Acta*. In the press.

STÅHL, K. & YMÉN, I. (1983). *Acta Chem. Scand. Ser. A*. In the press.

Acta Cryst. (1983). B**39**, 620–625

Packing Characteristics of the Aliphatic Chains in Bis(*n*-alkylammonium) Tetrachlorozincate(II) with Even and Odd Numbers of Carbon Atoms

BY F. J. ZUÑIGA AND G. CHAPUIS

Institut de Cristallographie, Université de Lausanne, BSP, 1015 Lausanne, Switzerland

(*Received* 22 *December* 1982; *accepted* 29 *April* 1983)

Abstract

The series of compounds $[(n\text{-}C_mH_{2m+1})NH_3]_2MCl_4$ crystallize in layers alternately formed by the metal complexes and the alkylammonium chains. They exhibit various phase transitions depending on the parity of the number of C atoms included in the chains. To compare the packing characteristics of even and odd members of the Zn series, the structure of $[(C_{13}H_{27})NH_3]_2ZnCl_4$ was solved. The structure is monoclinic, space group $P2_1$, M_r = 607·48, a = 10·644 (2), b = 7·3074 (9), c = 44·043 (7) Å, β =

0108-7681/83/050620-06$01.50